Fatigue crack initiation and growth behavior within varying notch geometries in the low-cycle fatigue regime for FV566 turbine blade material

Cunningham, B. M. D., Leering, M., Fan, Y., You, C., Morris, A., Reed, P. A. S., Hamilton, A. R. & Fitzpatrick, M. E.

ORIGINAL ARTICLE

FFEMS — Fatigue & Fracture of Engineering Materials & Structures

WILEY

Fatigue crack initiation and growth behavior within varying notch geometries in the low-cycle fatigue regime for FV566 turbine blade material

Benjamin M. D. Cunningham[1] | Mitchell Leering[2] | Yuhui Fan[3] | Chao You[3] | Andrew Morris[4] | Philippa A. S. Reed[1] | Andrew R. Hamilton[1] | Michael E. Fitzpatrick[2]

[1]Department of Mechanical Engineering, University of Southampton, Southampton, UK

[2]Faculty of Engineering, Environment, and Computing, Coventry University, Coventry, UK

[3]College of Energy and Power Engineering, Nanjing University of Aeronautics and Astronautics, Nanjing, China

[4]Coal & Gas Operations, Central Technical Organisation, EDF, Gloucester, UK

Correspondence
Benjamin M.D. Cunningham, Department of Mechanical engineering, University of Southampton, Southampton, UK, SO17 1BJ.
Email: b.cunningham@soton.ac.uk

Abstract

Plain bend bars made from FV566 martensitic stainless steel were extracted from the root of ex-service power plant turbine blades and several industry-relevant notch geometries were introduced. Some of the samples were shot peened. The notched bend bars were loaded plastically in the low-cycle fatigue regime and finite element (FE) modeling carried out to investigate the effects of changing notch geometry, combined with shot peening, on fatigue behaviors such as crack initiation, short crack growth, and coalescence. Shot peening damaged the notch surface, accelerating initiation behaviors, but had a lifetime-extending effect by retarding short crack growth in all tested notch geometries. At a total strain range higher than 1.2%, the lifetime extension benefit from shot peening was diminished due to compressive residual stress relaxation in the notch stress field. Notch geometry (and the associated varying constraint levels and stress/strain gradients) was found to have no notable difference on fatigue life when tested at identical notch-root strain ranges.

KEYWORDS
constant amplitude, low cycle fatigue, notch field, notches, short crack growth, stainless steel

Highlights

Initiation activity increased with increasing strain range regardless of notch geometry. Surface damage from the shot peening increased initiation activity and lowered a/c ratios. Shot peening reduced the early short crack growth rate at lower ΔK by a factor of 10. Shot peening increased lifetimes up to a strain range of 0.8%–1.2%.

1 | INTRODUCTION

The increased usage of less-predictable renewable energy sources has driven intermittent use of steam turbines to meet energy demand, resulting in steam turbine blades being increasingly exposed to cyclic fatigue conditions. Consequently, cracks have been observed via Non-Destructive Technique (NDT) methods during routine inspection in the fir-tree-root-fillets of in-service turbine blades.[1]

A service-life extension strategy known as the 'blend-polish-peen-repair' approach involving grinding out existing cracks from the fir-tree-root-fillets followed by shot peening was proposed and tested with the aim of extending the lifetime of U-notched three-point bend bar samples.[2] Grinding out existing cracks alters the depth and radius of the notch (Figure 1A), which may be expected to reduce fatigue life. In contrast, the fatigue process is temporarily repressed, requiring crack initiation and short crack growth to reoccur, consequently extending service life. Additionally, shot peening the notch surface will introduce residual compressive stress and work-hardening in the notch surface region, offering additional fatigue resistance. Thus a fuller evaluation of the overall benefits and factors operating over the notch fatigue process in such a scenario is required.

It is well known that a notch redistributes stress flow, creating an area of localized stress (above nominal stress) on and beneath the notch center surface or root, known as the notch field (Figure 1B). The effect of notch geometry on the maximum stress experienced on the notch surface, based upon elastic material assumptions, is well quantified and understood.[3] While elastic material behavior assumptions may be reasonable for the high-cycle fatigue regime, low-pressure turbine blades often operate in the low-cycle fatigue regime, where stresses typically approach or surpass the yield strength of the material. It is important to understand how material plasticity affects the distribution of stress and strain within the notch field, explored by Liao et al.[4] (Figure 1C). The stress at the notch surface is close to the yield stress of the material with the maximum stress typically seen some depth beneath the surface due to 'notch constraint' effects of surrounding material.

FV448 U-notched samples with a typical notch geometry representative of turbine blade fir-tree-root-fillets
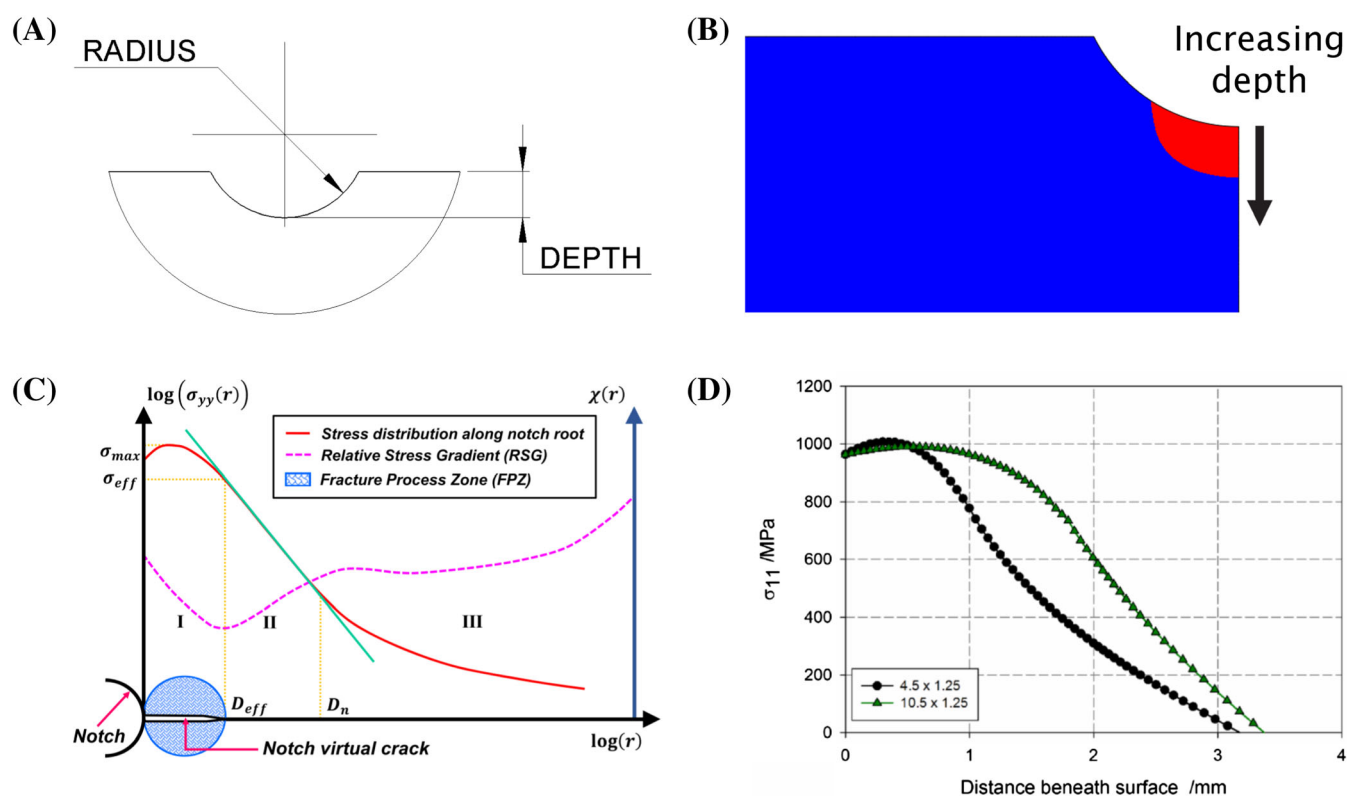

FIGURE 1 (A) A schematic identifying the depth and radius of a typical U-notch geometry. (B) A schematic showing the notch field shown in red with elevated stress levels above the nominal stress (or far field) stress, shown in blue. (C) Stress distribution versus notch depth based upon elastic–plastic material behavior assumptions (with no crack present shown as the red line) from Liao et al.[4] (D) Longitudinal stress versus depth beneath notch surface showing the stress distribution within the notch field for U-notched specimens made from FV448 with notch depth of 1.25 mm and notch radii of 4.5 and 10.5 mm.[5] [Colour figure can be viewed at wileyonlinelibrary.com]

were analyzed using finite element modeling, accounting for material plasticity and hardening behavior.[5] Increasing the notch radius from 2.25 to 5.25 mm, while maintaining the same maximum tensile strain at the notch root surface resulted in a slightly reduced maximum stress and a notch field that penetrated deeper beneath the notch surface (Figure 1d).

Changing notch geometry therefore changes the distribution of stress range and strain range within the notch field during cyclic loading, potentially altering fatigue behavior. There is scope to extend our current understanding of how changing notch geometry affects the distribution of stress and strain within the notch field accounting for material plasticity behavior. In particular, stress and strain range distribution, residual stress distribution after unloading, and residual stress relaxation effects after shot peening.

Shot peening is frequently used on localized areas such as the fir-tree-root-fillets of low-pressure turbine blades to improve fatigue resistance.[6–8] Shot peening can induce surface strain hardening to approximately 150 μm and compressive residual stress to approximately 500 μm beneath the notch surface. Increased dislocation density may limit the movement of persistent slip bands (PSBs) inhibiting crack initiation, while the compressive residual stress produced by the plastic deformation at the surface reduces the effective mean stress, increasing resistance to fatigue crack propagation.[2,5–11] Conversely, shot peening also increases surface roughness, which is considered detrimental to fatigue due to the presence of local stress concentration features which induce earlier crack initiation.[12]

Additionally, for relatively extreme Low-Cycle Fatigue (LCF) conditions (<10,000 cycles), the application of relatively high strain ranges (>1%) can relax the compressive residual stress produced from shot peening within the first 1% of fatigue life for FV448 material.[5,9,13–15] With a diminished compressive residual stress field, the retardation effect from shot peening on short crack propagation is no longer apparent. Studies have shown that the benefits of shot peening outweigh the drawbacks for the majority of fatigue situations, resulting in an improved resistance to fatigue overall, including for in-service turbine blades in low-cycle fatigue conditions.[2,5,14]

This paper therefore uses a systematic finite element analysis study to investigate how changing the notch geometry may affect the stress and strain range distribution within the notch field after one loading cycle followed by the corresponding residual stress distribution after unloading. Additionally, the effect of changing the notch geometry on residual stress relaxation following shot peening was explored. Experimental testing on polished and shot peened FV566 martensitic stainless-steel samples with various U-notch geometries was

carried out to better understand the impact of changing notch radius and depth on fatigue behavior, and to compare with the modeling results. U-notched specimens were subjected to typical LCF conditions, where material plasticity, strain hardening, and residual stress are expected to influence lifetimes. A surface replication technique was used to observe the surface of the notch at regular cyclic intervals to investigate initiation, short crack growth, and coalescence behaviors. This work will therefore allow a better understanding of the impact notch geometry may have during the application of the proposed blend-polish-peen repair service-life extension strategy.

2 | MATERIALS AND EXPERIMENTAL METHOD

The material used in this study is FV566 martensitic stainless steel extracted from the roots of ex-service low-pressure steam turbine blades as bend bars. It is understood that this material has been austenitized at 1050°C, oil quenched, followed by tempering at 650°C.[16] The material microstructure, material properties and baseline fatigue behavior are reported in our previous work.[1]

Plain bend-bars made from FV566 were extracted from two ex-service turbine blades and U-notched with varying depths and radii machined in the center of the sample (Figure 2A). The notch surfaces of all U-notch samples were polished with a rotary tool using 9-μm polishing suspension to remove machining marks. The polishing process removed less than 1 μm from the notch profile. The depth and radius of the notch geometries were measured to 1-μm accuracy after polishing using optical microscopy and image post-processing software (Figure 2B).

The U-notch surface and corresponding top surface of some of the U-notch samples were then shot peened with a T0 industrial standard shot peen (MI230R 200% 13A) by Sandwell UK Ltd. The shot diameter was 0.58 mm, shot hardness (Hardness Rockwell C) 45–52 HRC and shot velocity was 57 m s^{-1}.

Surface roughness R_a measurements of polished (Figure 2C) and shot peened (Figure 2D) U-notch surfaces were taken using a profilometer (Infratouch) in accordance with BS EN ISO 21920-3:2022[17] in the traverse direction (perpendicular to the tensile axis) for all notch surfaces with a measurement length of 5 mm and Lc value of 0.8.

X-ray diffraction (XRD) using a Stresstech Xstress Robot was carried out by Coventry University, on a shot-peened U-notch sample with notch radius of 2.25 mm and notch depth of 1.5 mm to obtain residual stress

FIGURE 2 (A) Drawing for a typical U-notched plain bend-bar sample showing notch radius and depth, all dimensions are in mm. (B) The final measured U-notch geometries subject to experimental testing. (C) Optical microscopy images of the polished notch surface condition for turbine blade surfaces and (D) the T0 shot peened surface condition. (E) X-ray diffraction (XRD) measurements in the longitudinal and transverse directions were taken at three locations on the flat surface and on the notch center surface by Coventry University. [Colour figure can be viewed at wileyonlinelibrary.com]

profiles using an incremental layer removal method. XRD was carried out in the longitudinal direction and transverse direction at three locations on a U-notched surface and flat surface totaling six tests (Figure 2E). The XRD equipment was calibrated and validated on stress-free Fe powder. A collimator diameter of 0.5 mm was used with exposure time of 20 s over 12 tilts from $-45°$ to $45°$. The peak diffraction angle was found to be 156.4°. A daily zero reading was taken which was used to determine measurement error. An exposure time of 50 seconds with tilt oscillation of 0° was used. Each layer was removed using an electro-polishing method (Struers

—WILEY—

LectroPol) with A2 electrolyte, a mask of 0.5 mm^2, 20 V flow rate setting of 14 for 12 s.

A 3D nonlinear finite element quarter model was developed using ABAQUS[1] to determine test loading conditions and provide strain range estimations in the center of the notch.[1] C3D20 full integration quadratic hexahedral elements were used. A mesh convergence study was carried out to determine an adequate mesh.[18] Elastic–plastic material data from monotonic tensile testing performed by Frazer-Nash Consultancy (FNC)[1] was used to describe the plastic behavior of the material. This model was used to identify the loads P_{max} and P_{min}
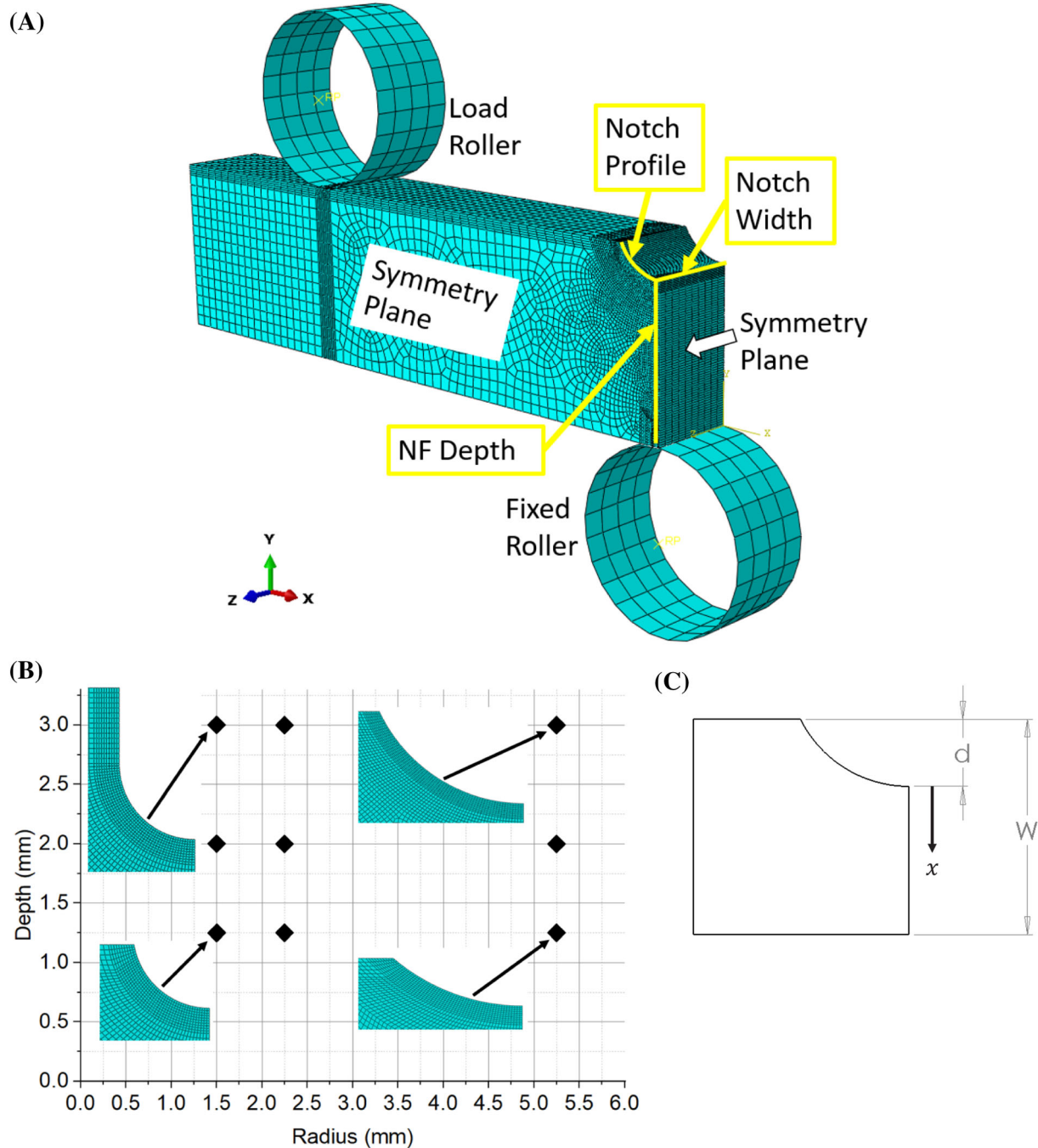
FIGURE 3 (A) An ABAQUS quarter model of a typical U-notch sample. The longitudinal stress and total strain were obtained along the notch field (NF) depth, notch profile, and notch width locations outlined by the yellow lines. (B) Notch depth versus notch radius for various notch geometries using the ABAQUS quarter model. (C) Schematic depiction of the variables for calculating normalized notch stress depth where W is sample depth, d is notch depth, and x is increasing notch field depth in (mm). [Colour figure can be viewed at wileyonlinelibrary.com]

required to produce total strain ranges of 0.75%, 1.15%, and 1.65% at the notch root surface based upon an R-ratio of 0.1 for all notch geometries (Figure 3B). The longitudinal stress range ($\sigma_{max} - \sigma_{min}$) and longitudinal total strain range ($\varepsilon_{max} - \varepsilon_{min}$) along the notch field depth, notch profile, and notch width highlighted by yellow lines in Figure 3A were obtained for each notch geometry. A linear unloading step from P_{max} to 0 N was carried out and the residual stress in the longitudinal direction along the notch field obtained for all notch geometries. The notch field depth was normalized (Figure 3C and (Equation 1)) to allow similitude and

direct comparison of the notch field with notch geometries of various notch depths.

$$Normalised\ Depth = \frac{x}{W - d} \quad (1)$$

Fatigue testing was carried out under three-point bend loading conditions on U-notch samples, as shown in Figure 2A, on an Instron TM ElectroPulse E10000 Electromechanical fatigue testing machine at room temperature using a sinusoidal waveform at 10-Hz frequency
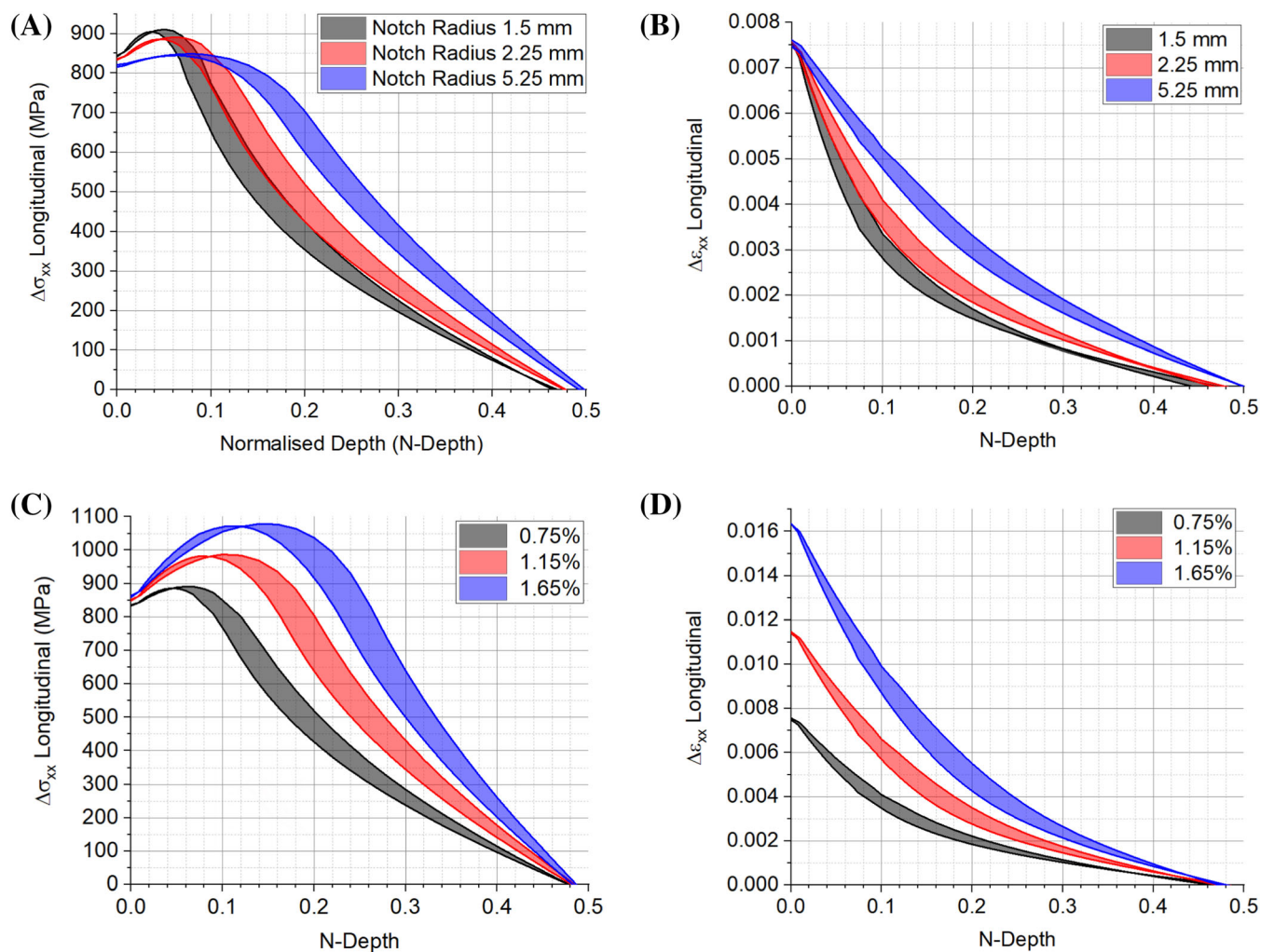
FIGURE 4 FEA showing the effect of (A) increasing notch radius from 1.5 to 5.25 mm on stress range as a function of normalized depth for applied strain range of 0.75%. (The shaded bands indicate the spread of distribution with notch depths ranging from 1.5 mm to 3 mm). (B) Increasing notch radius from 1.5 mm to 5.25 mm on strain range as a function of normalized depth for applied strain range of 0.75%. (The shaded bands indicate the spread of distribution with notch depths ranging from 1.5 mm to 3 mm). (C) Increasing strain range at the notch Centre on the stress as a function of normalized depth with a constant notch depth of 2.25 mm. (The shaded bands indicate the spread of distribution with notch depths ranging from 1.5 to 3 mm). (D) Increasing strain range at the notch center on the strain range distribution within the notch field with a constant notch depth of 2.25 mm. (The shaded bands indicate the spread of distribution with notch depths ranging from 1.5 to 3 mm). [Colour figure can be viewed at wileyonlinelibrary.com]

at a baseline R-ratio of 0.1. Continuous fatigue testing was carried out on U-notch samples to obtain representative lifetimes for various notch geometries, surface conditions and strain ranges (0.75%, 1.15%, and 1.65%). Interrupted fatigue testing was carried out on U-notch samples involving regular surface replication of the notch root using Repliset-F5 (Struers Ltd) silicone with a resolution of 10 μm. This allowed the recording of crack initiation and growth mechanisms in the surface of the U-notch at regular intervals during fatigue cycling.

A record of crack length, *cproj*, versus number of cycles, *N*, was constructed for short crack growth rate determination. Crack growth rates d*cproj*/d*N* were calculated using the secant method and compared for the U-notch specimens tested. The ΔK values of the short cracks were calculated using the methodology described in previous works.[19,20]

3 | RESULTS

The polished notch surfaces had an average R_a surface roughness of 0.039 μm $\pm$ 0.015 μm (one standard deviation). The shot peened notch surfaces have a surface roughness R_a of 2.7 μm $\pm$ 0.4 μm (one standard deviation).

The typical stress range distribution with notch field depth shows an increase in stress range below the notch surface to a maximum stress range between normalized depth between 0.04 and 0.14. This is followed by a decrease in the stress range as the normalized depth approaches the neutral axis at approximate notch field depth between 0.45 and 0.5 due to bending loading conditions (Figure 4A). The typical strain range distribution with normalized depth initially shows a rapid decrease somewhat linearly until between 0.06 and 0.15 normalized depth. The rate at which the strain range decreases with normalized depth decreases gradually until between 0.2 and 0.35 notch field depth. The strain range then decreases linearly until a zero strain range is observed at the neutral axis (Figure 4B).

At a strain range of 0.75% at the notch surface, increasing the notch depth from 1.5 to 3 mm resulted in a small increase in the maximum stress range which was shifted deeper into the notch field. At normalized depth of 0.1, changing the notch depth from 1.25 to 3 mm resulted in the largest stress range difference of 125 MPa (Figure 4A) and the largest strain range difference of 0.075% which was independent of notch radius (Figure 4B).

Increasing the notch radius from 1.5 to 5.25 mm resulted in a decrease in the maximum stress range from

approximately 900 to 850 MPa, which was shifted deeper into the notch field from normalized depth of 0.05 to 0.08 (Figure 4A). The strain range distribution shifted toward a linear relationship with increasing notch radius (Figure 4B).

Increasing the applied strain range from 0.75% to 1.65% for a constant notch radius of 2.25 mm only slightly increased the stress range at the notch surface by 20 MPa due to material plasticity (Figure 4C). The stress range and strain range were almost doubled between a normalized depth of 0.15 and 0.2 from the notch surface. The stress and strain range distribution and overall size of the notch field increased more significantly than changing the notch geometry alone for the geometries and surface strain ranges tested (Figure 4C,D).

A typical residual stress profile predicted from the Finite Element Analysis (FEA) following unloading from P_{max} of 0.81% notch surface strain on a 1.5-mm radius by 1.25 mm depth notch geometry shows a maximum compressive residual stress at the notch surface of approximately 440 MPa. The residual stress decreases rapidly at a near linear rate until 0.04 normalized depth where no residual stress was seen. This is then followed by a counterbalancing maximum tensile residual stress of 100 MPa at 0.07 normalized depth. The residual stress then decreases at a decreasing rate, tending toward a zero residual stress at the neutral axis (Figure 5A).

Increasing notch depth from 1.5 to 3 mm slightly decreases the maximum compressive residual stress at the notch surface. The crossover from compressive to tensile residual stress was shifted deeper into the notch field as was the slightly increased maximum counterbalancing tensile residual stress. Increasing notch radius from 1.25 to 5.25 mm resulted in a larger maximum compressive residual stress at the notch surface. The crossover from compressive to tensile residual stress was shifted deeper from the notch, as was the increased maximum compressive residual stress (Figure 5A). Increasing P_{max} and therefore strain at the notch surface increased the residual stress field overall more significantly than changing the notch geometry alone for the geometries and surface strain ranges tested (Figure 5B).

The residual stress distribution in the shot peened notched sample (2.25 mm × 1.25 mm) was reconstructed by applying the inverse eigenstrain method introduced in You et al.[15] The residual stress profile in depth, which was obtained using XRD, was applied as an input for the modeling. The relation between the longitudinal (ε_{xx}) and transverse (ε_{yy}) eigenstrain components was determined to be $\varepsilon_{xx} = 1.1\varepsilon_{yy}$. Figure 6 shows the comparison between the reconstructed residual stress profile and the measured one at the bottom of the notch. The advantage of this modeling method is that although only limited
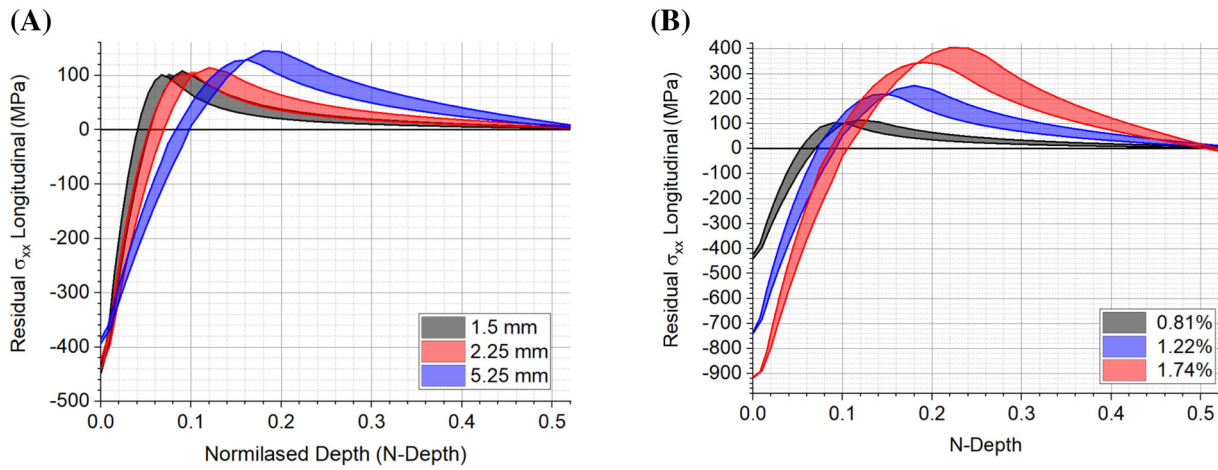
FIGURE 5 FEA results of the distribution of residual stress in the longitudinal direction after unloading from P_{max} with increasing normalized depth from the notch surface (N-Depth) for (A) increasing notch radius on residual stress distribution within the notch field for strain range of 0.81% applied at the notch center (the shaded regions show the range of residual stress distributions of notch depths between 1.25 and 3 mm), (B) increasing strain range at the notch center on the residual stress distribution within the notch stress field for notch radius of 2.25 mm. (The shaded regions shows the range of residual stress distributions from notch radii between 1.5 and 5.25 mm). [Colour figure can be viewed at wileyonlinelibrary.com]
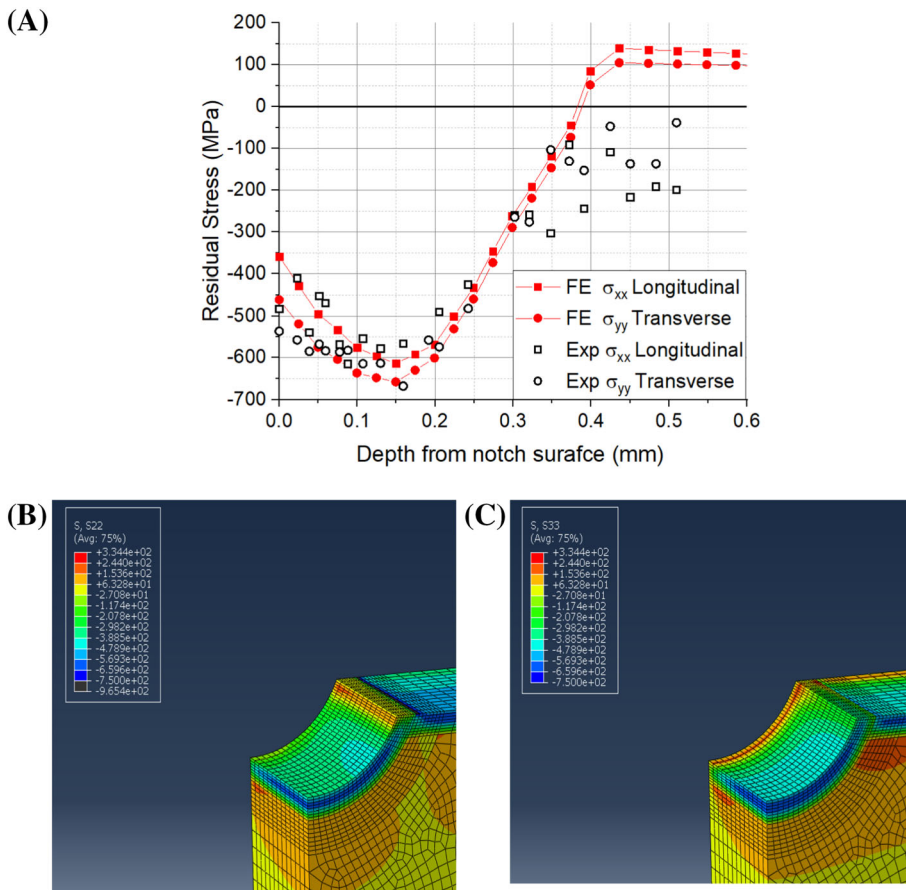
FIGURE 6 (A) Comparison between the reconstructed residual stress and the X-ray diffraction (XRD) measured results at the bottom of the notch (2.25 × 1.25 mm) treated with shot peening. (B) Finite element (FE) longitudinal residual stress distribution within the notch. (C) FE transverse residual stress distribution within the notch. [Colour figure can be viewed at wileyonlinelibrary.com]

—WILEY—

residual stress data can be obtained from XRD measurements, the full residual stress distribution can be reconstructed (as shown in Figure 6), providing comprehensive residual stress information for subsequent fatigue analysis.

The FE model containing the reconstructed residual stress induced by shot peening was used to estimate the expected residual stress relaxation behavior under cyclic loading. Three cyclic load levels (1 cycle) with corresponding notch root strain ranges of 0.75%, 1.15%, and 1.65%, respectively, were applied in the model. As a comparison, the same cyclic loading schemes were also applied to the FE model without shot peening effects (i.e., the un-peened condition) to simulate the residual stress distribution resulting purely from bending. The modeling results are demonstrated in Figure 7A,B. It can be seen that greater longitudinal compressive residual stresses are generated

near the surface in the un-peened samples at higher load levels. In addition, the longitudinal residual stress is hardly relaxed by external loads, and conversely, tends to be enhanced. This phenomenon is attributed to the increased mismatch of the eigenstrain caused by bending, as elucidated in You et al.[15] The diminished gap between the residual stresses in shot-peened and un-peened samples implies that the benefits of shot peening in maintaining compressive residual stresses near the surface becomes less effective at higher load levels.

The same modeling process was repeated for the 1.5 × 2 notched sample (the repaired notch) and the results are shown in Figure 7C,D. The applied load levels give the same strain range at the notch root with those for the 2.25 × 1.25. Similar trends and residual stress distributions with Figure 7A,B are obtained.
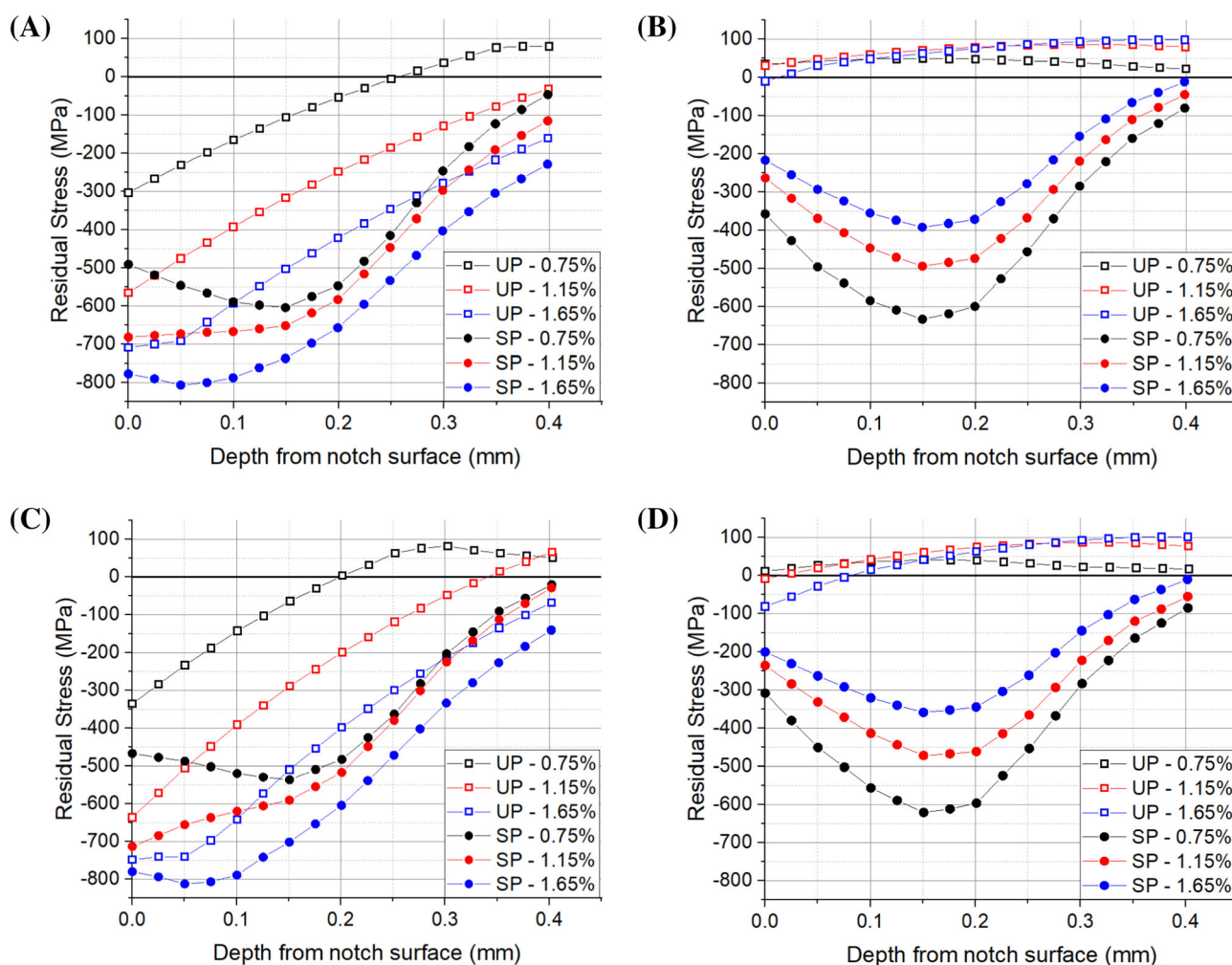
FIGURE 7   Comparison of the simulated residual stress relaxation behavior in shot-peened (SP) and un-peened (UP) notched samples under different load levels for (A) longitudinal and (B) transverse residual stress components for notch geometry of 2.25-mm radius and 1.25-mm depth and (C) longitudinal and (D) transverse residual stress components for notch geometry of 1.5-mm radius and 2-mm depth. [Colour figure can be viewed at wileyonlinelibrary.com]

The number of crack initiation events forming the primary crack in various notch geometries and plain bend bars were plotted against applied strain range during post-test analysis (Figure 8A–C). Increasing the strain range tended to increase the number of crack initiation events on all notch geometries including plain bend bars, as expected. Changing both the notch radius and depth did not appear to have a clear impact on the number of crack initiation events. Plain bend bars (from FV448) tended to have a lower number of crack initiation events than notched samples, especially with increasing strain ranges.

The short crack growth rate versus $\Delta K_{Surface}$ for three samples with different notch geometries and surface conditions with longitudinal strain range of 0.75% were compared under linear elastic fracture mechanics (LEFM)

assumptions. The short crack growth rate versus $\Delta K_{Surface}$ behavior is minimally affected by a relatively small change in notch geometry (2.25-mm radius and 1.25-mm depth, and 1.5-mm radius and 3-mm depth) (Figure 9A).

On the other hand, T0 shot peening affected the short crack growth rate which was initially similar to polished surface condition at low $\Delta K_{Surface}$ values between 5 and 6 MPam$^{0.5}$. The compressive residual stress from shot peening slightly decreased growth rates with increasing $\Delta K_{Surface}$ values until 20 MPam$^{0.5}$ where crack growth rate was 10 times slower than the polished notch surface condition. The crack growth rate then rapidly increased toward polished surface condition levels possibly due to the expected counterbalancing tensile residual stress until 30 MPam$^{0.5}$ where coalescence events took over short crack growth behavior. While LEFM does not capture
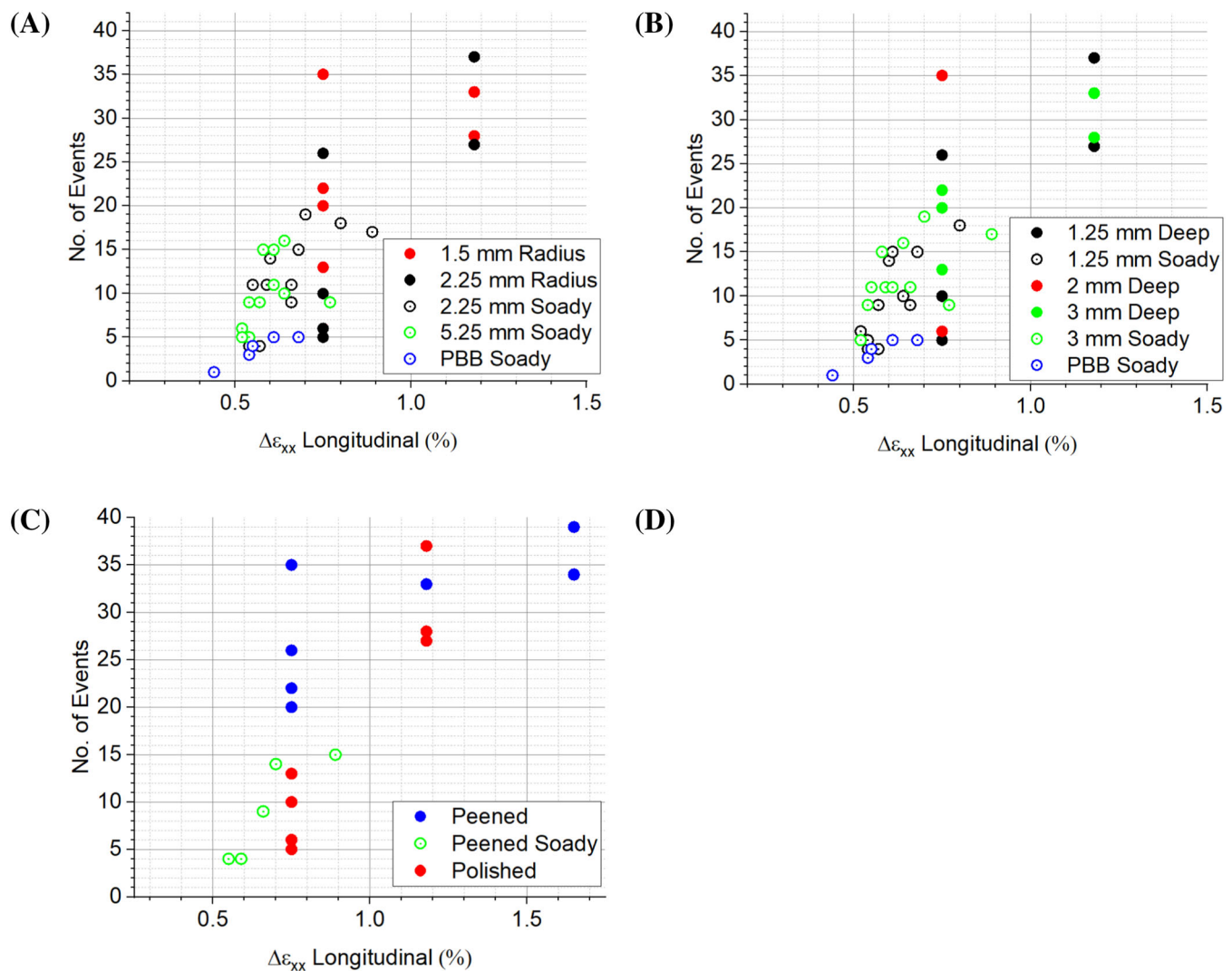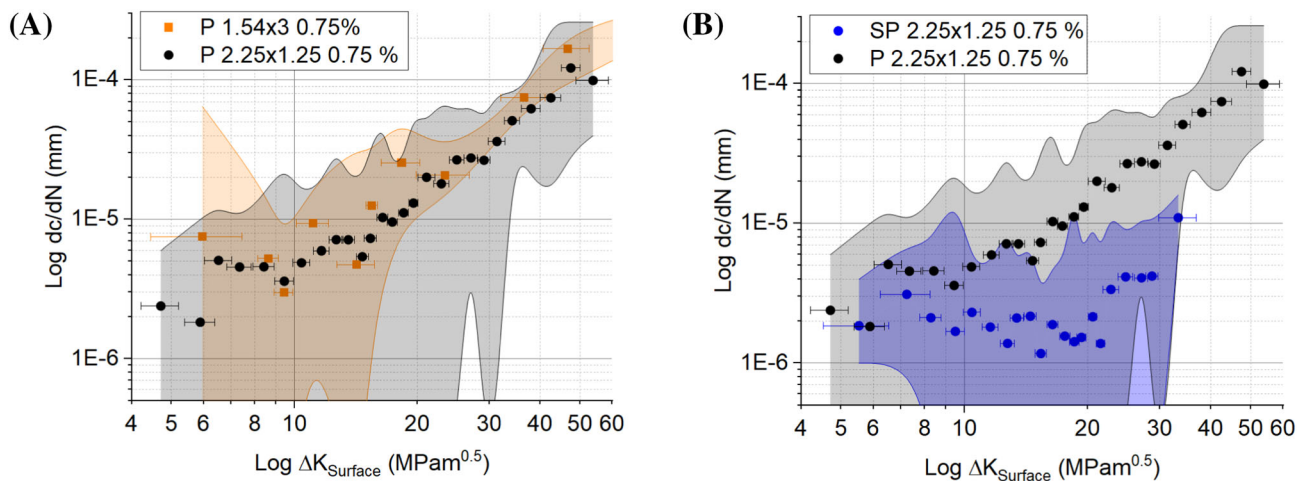

FIGURE 8 The number of initiation events versus total longitudinal strain range for (A) varying notch radius, (B) varying notch depth, and (C) notch surface condition. The results include FV448 from Soady.[5] [Colour figure can be viewed at wileyonlinelibrary.com]

FIGURE 9   (A) The average short crack growth rate dc/dN versus $\Delta K_{Surface}$ for each $\Delta K_{Surface}$ group for (A) two polished notch surfaces with different notch radius and depth and (B) polished and T0 shot peened notch surface conditions with a typical notch geometry. The shaded regions represent the maximum and minimum dc/dN values for each $\Delta K_{Surface}$ group. [Colour figure can be viewed at wileyonlinelibrary.com]

effects of plasticity, especially at lower ΔK values for LCF conditions, it is nonetheless evident that a variation in notch geometry minimally affected short crack growth rates, while shot peening had a large crack growth rate retardation effect.

A detailed study of the short crack growth behavior of the primary crack using a similar method detailed in Cunningham et al.[1] was carried out for U-notch specimens with a notch geometry of increased depth and reduced radius, increased strain range at the notch surface, and with a T0 shot peened notch surface. The number of crack initiation events (adding to the total number of cracks that made up the primary crack) and coalescence events (subtracting from the total number of cracks that made up the primary crack) for several samples are presented in Figure 10A–D. To gain further understanding and visualization of the crack initiation coalescence and growth stages, a PowerPoint animation approach was used to reconstruct the evolution of the short cracks from the silicone replicas to scale (Figure 10E–G).

Increasing notch depth and decreasing notch radius resulted in a particularly dominant crack that produced a large area of shielding and plastic zone of heightened strain ahead of the crack tip, inducing crack initiations to form in the path of the dominant crack. The propagation mechanism predominantly featured the dominant crack encompassing smaller cracks in the form of in-plane coalescence (Figure 10A,D,E). The video can be viewed here https://www.youtube.com/watch?v=uyD2Pd4gs5E and also at https://eprints.soton.ac.uk/476501/. Changing the strain range reduced the overall number of cycles to

failure but did not appear to significantly change crack initiation, propagation or coalescence behavior (Figure 10B,D,F. The video can be viewed here https://www.youtube.com/watch?v=kE3UmSUmPzk) and also at https://eprints.soton.ac.uk/476501/. Shot peening the notch surface led to rapid crack initiation and coalescence initially, followed by a prolonged period of very slow crack growth with very low initiation and coalescence activity. (Figure 10C,D,G). The video can be viewed here https://www.youtube.com/watch?v=2MS0NIYdje8 and also at https://eprints.soton.ac.uk/476501/. Late fatigue behavior is typically dominated by high coalescence activity until the main crack has grown the width of the sample followed by long crack growth to failure regardless of notch geometry, loading, or notch surface conditions.

Semi-elliptical fatigue regions indicating short crack growth were identified on the fracture surfaces of polished and shot peened U-notched samples and the a/c ratios presented along with results from He et al.[10] and theoretical equilibrium ΔK values around the perimeter of the semi-ellipse.[10,11]

The a/c ratios for a polished notch surface were between 0.7 and 0.8 with longer crack lengths having slightly higher a/c ratio than theoretical equilibrium. The results from He et al.[10] for a polished sample tended to be higher with a/c ratios of 0.95 or 1.15. The shot peened sample showed much more variation in a/c ratios than the polished surface condition. Four main clusters were observed with a/c ratios of 1.2, 0.8–0.9, 0.6, and 0.25–0.4, similar to results from He et al.[10]
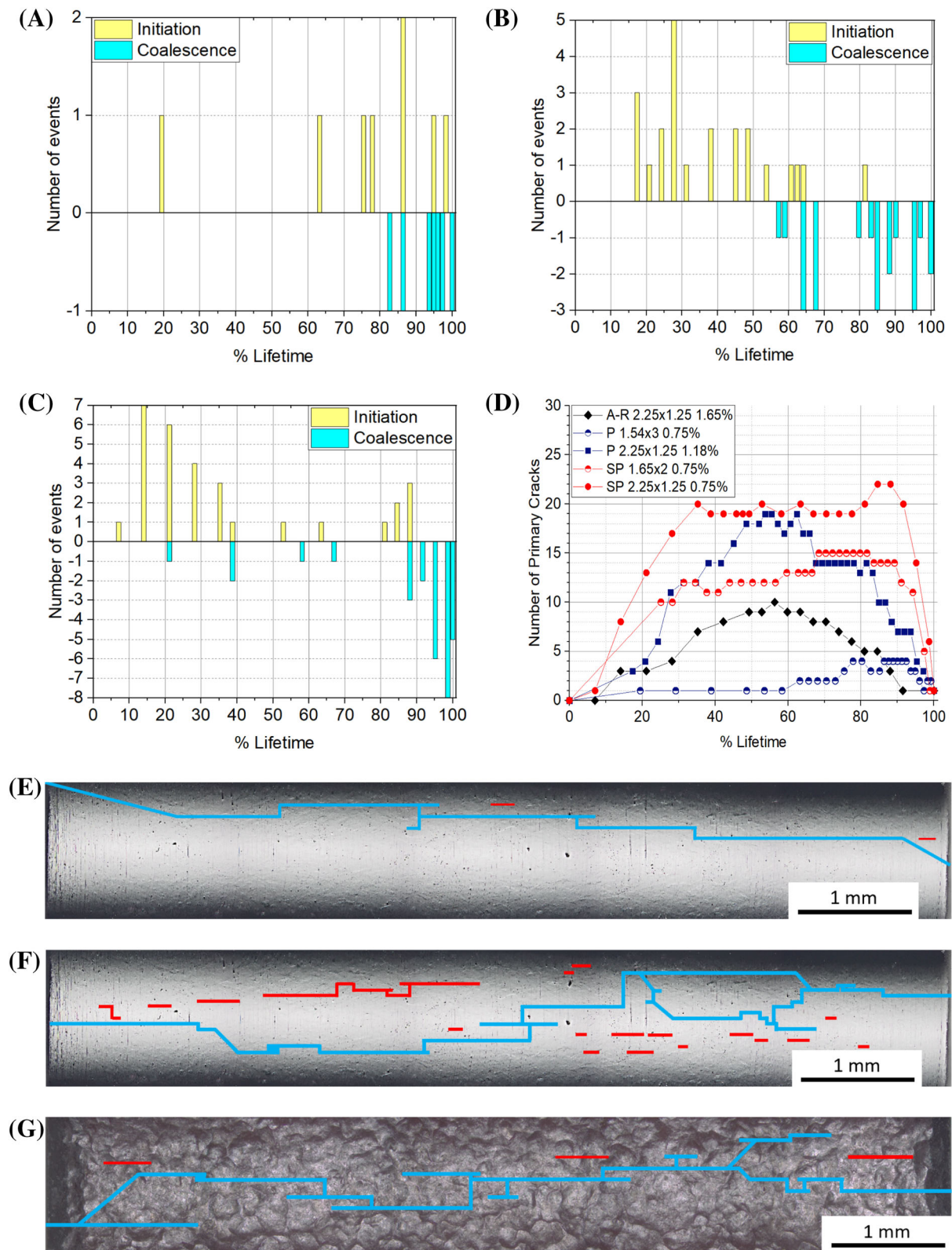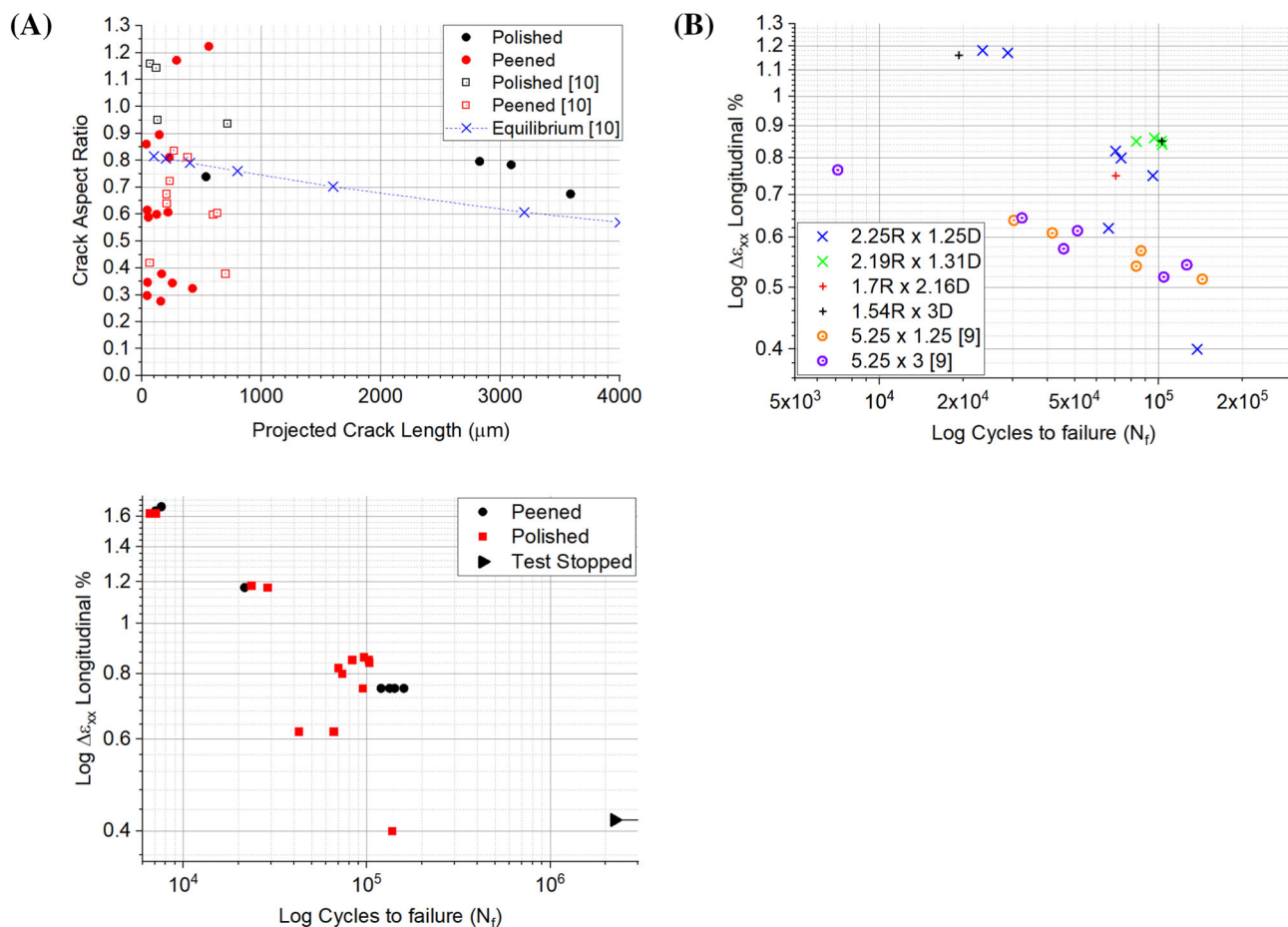
FIGURE 10 Legend on next page.

(A)

(B)

FIGURE 11 (A) Crack aspect ratio (*a/c*) versus crack length for polished and shot peened notch surface conditions. A theoretical equilibrium *a/c* ratio is included from He et al.[10] for comparison. Longitudinal strain range at the notch surface versus number of cycles to failure for (B) U-notched samples with various notch radii (*R*) and notch depths (*D*). Hollow circles show results from FV448.[9] (B) U-notched samples with polished and shot peened notch surface conditions including a test stopped after 2,250,000 cycles due to a lack of initiation activity. [Colour figure can be viewed at wileyonlinelibrary.com]

Varying the notch radius and notch depth of U-notched samples made from both FV566 and FV448[9] (with less resistance to the application of cyclic fatigue), minimally impacted their fatigue lifetimes, no observable relationship between notch radius and notch depth and fatigue lifetime is observed in the data provided (Figure 11A).

At relatively low strain ranges (0.8% or less) a T0 shot peen to the notch surface tends to increase fatigue lifetime over polished samples. At 0.4% notch surface strain

FIGURE 10 The number of initiation events in yellow (adding to the number of primary cracks) and coalescence events in blue (subtracting from the number of primary cracks) formed in between each replica for (A) polished notch surface with notch radius of 1.54 mm and notch depth of 3 mm at a strain range of 0.75%, (B) polished notch surface with notch radius of 2.25 mm and notch depth of 1.25 mm at a strain range of 1.18%, (C) T0 shot peened notch surface with notch radius of 2.25 mm and notch depth of 1.25 mm at a strain range of 0.75%. (D) The total number of cracks that made up the primary crack versus percentage lifetime for samples with different surface conditions, notch geometries, and strain ranges. (E) The final notch surface replica record from the crack evolution diagrams for polished notch surface with notch radius of 1.54 mm and notch depth of 3 mm at a strain range of 0.75%, (F) polished notch surface with notch radius of 2.25 mm and notch depth of 1.25 mm at a strain range of 1.18%, and (G) shot peened notch surface with notch radius of 2.25 mm and notch depth of 1.25 mm at a strain range of 0.75%, where blue indicates coalescing cracks and red indicates cracks that arrested. [Colour figure can be viewed at wileyonlinelibrary.com]

range, a polished sample failed at approximately 137,400 cycles, whereas no cracks were observed on the shot peened sample at 2,240,000 cycles, where the test was subsequently stopped before failure. At strain ranges above 1.2%, the fatigue lifetime of shot peened samples were equivalent to polished counterparts at which point the lifetime extending effect of shot peening was clearly diminished (Figure 11B).

4 | DISCUSSION

The typical longitudinal stress distribution within the notch field was similar to that presented in Liao et al.[4] A 3D FE model was compared with a 2D model using plane stress elements. 2D modeling resulted in an overestimation of the distribution of stress and strain within the notch field due to the assumption of an infinite width geometry (Figure 12D). Increasing notch depth had the least impact on the notch field, followed by notch radius with strain range at the notch having the greatest impact on notch field size. Depending on the sample/component geometry, changing the notch depth could influence the applied strain range experienced at the notch surface under more force-controlled loading conditions. Therefore, the influence of notch depth on stress concentration factor is clearly sample-geometry-dependent and needs to be evaluated carefully in component structural integrity assessments.

The XRD performed on the U-notch surface of T0 shot peened samples suggested a higher compressive residual stress in the longitudinal direction than the transverse direction. While a measurement angle of ±45°
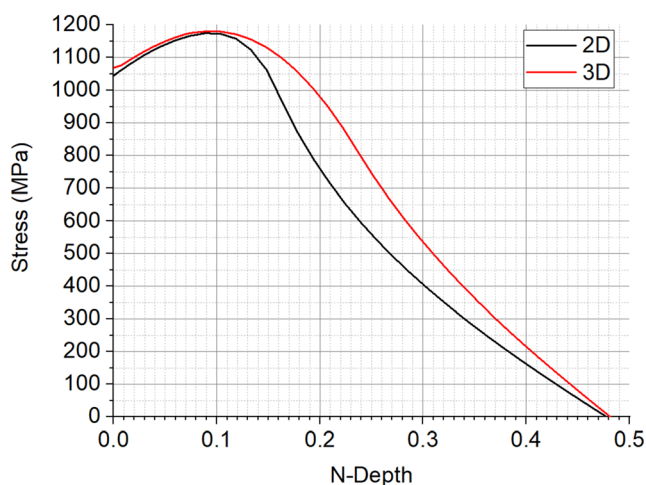

FIGURE 12 A comparison between 2D plane stress finite element (FE) modeling and 3D FE modeling of the notch field stress distribution as normalized depth. [Colour figure can be viewed at wileyonlinelibrary.com]

was achieved in the transverse direction, the longitudinal direction was limited to ±30° due to shadowing effects from the notch geometry. As a result, the limited angle range reduced the d-spacing range which predicted a smaller residual stress profile (Figure 13A). Additionally, XRD carried out on the flat shot peened surface allowed a full 45° measurement range in both directions and so improved accuracy (Figure 13B). The similarity in residual stress profiles suggests minimal effect from material anisotropy and a minimal difference between the notched and flat surfaces.

The compressive residual stress from a similar T0 shot peened U-notch surface with identical dimensions was obtained via XRD in FV448 material.[9] Accounting for the presumed conservative residual stress result in the longitudinal direction for FV566, FV448 suggests a larger compressive residual stress despite the reduced material strength (Figure 13C,D). Surface roughness results suggest that a harsher T0 shot peening process may have been applied to the U-notch surface of the FV448 material, which may result in a larger compressive residual stress observed overall.[21,22]

Increasing the strain range at the notch surface increased the number of crack initiation events regardless of surface condition or notch geometry. The effect of changing the notch radius or depth on number of crack initiation events could not be determined due to intervening variables such as differences in material, notch geometry, and surface conditions. An as-received notch surface (with corrosion pitting) typically had a lower number of crack initiation events, possibly due to the onset of early initiation activity and growth behavior inhibiting later crack initiation due to shielding effects.[1] The shot peened notch surface typically had more crack initiation events than a polished or as-received notch surface, especially at lower strain ranges due to the presence of pre-existing cracks before testing (Figure 14), a feature seen in similar shot peened steels.[6,23,24]

The number of crack initiation events observed on a shot peened U-notch surface made from FV448 with applied strain ranges between 0.6% and 0.9%[10] were almost doubled when assessed in the FV566 at the same strain range. This difference can be attributed to the method used to count the number of initiation events on the surface. The number of crack initiation events for FV448 was found by backtracking replica records. An optometry surface profiling microscope was used to identify ratchet marks on the fracture surface of FV566 samples to estimate the number of initiation events.[18] The more tortuous short crack growth in the shot peened surface condition (also observed by He[2]), resulted in higher error and possible overestimation in the number of crack initiation events observed.
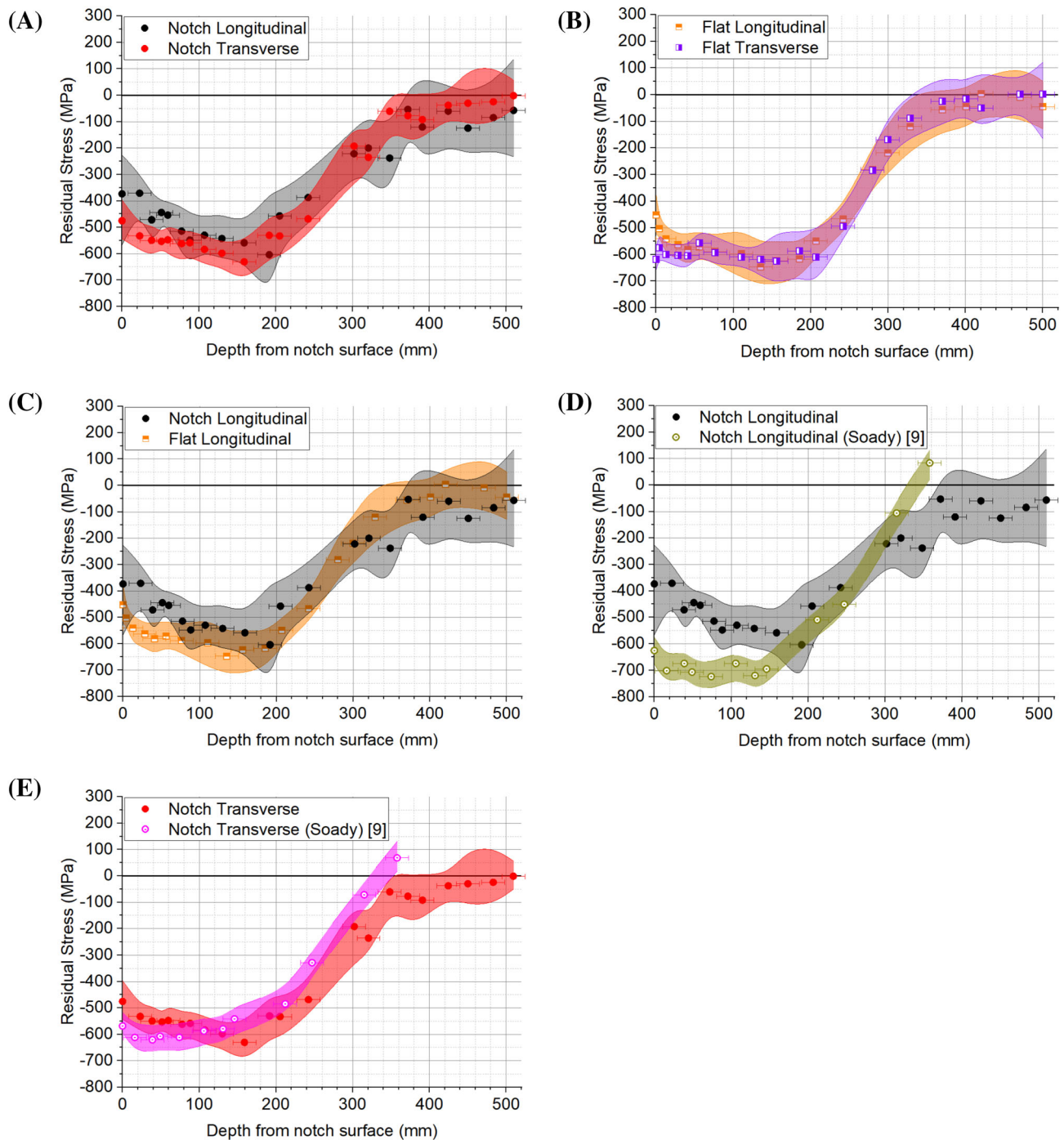
FIGURE 13 Residual stress profiles for FV566 samples for (A) the T0 shot peened notch in the longitudinal and transverse directions, (B) the T0 shot peened flat surface of the same sample in the longitudinal and transverse directions, and (C) the comparison between the flat and notched surface in the longitudinal direction. Residual stress profiles for (D) the T0 shot peened notch in the longitudinal direction for FV566 and FV448[9] and (E) the transverse direction. The shaded regions show the expected error range based upon testing at three locations and additional measurement error from daily zero readings. [Colour figure can be viewed at wileyonlinelibrary.com]

Despite notch geometry affecting stress and strain range distribution in the notch field, interrupted lifetime testing revealed that changing notch geometry did not significantly affect the short crack growth rate versus $\Delta K_{Surface}$ relationship based upon LEFM assumptions.

Similarly, changing notch geometry minimally altered overall fatigue crack growth behavior for the notch geometries and applied strain ranges tested.

Shot peening increased surface roughness and resulted in pre-existing cracks leading to early short crack
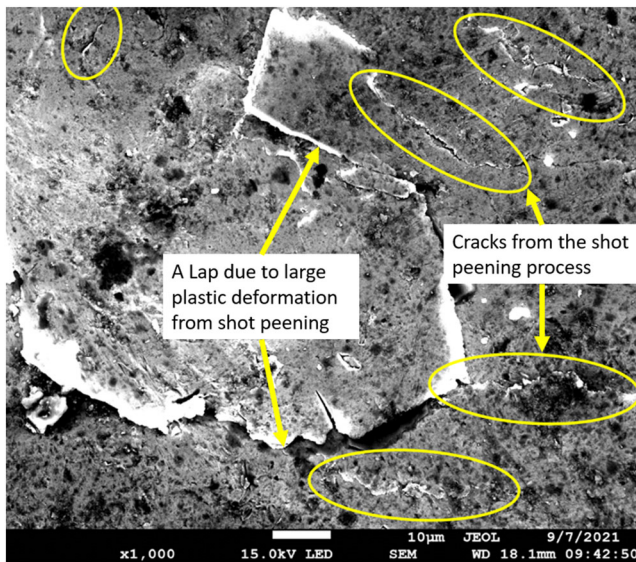
FIGURE 14 Annotated SEI image showing deformation and pre-existing cracks on the notch surface due to the shot peening process. [Colour figure can be viewed at wileyonlinelibrary.com]

initiation and coalescence behavior with low a/c ratios and therefore a preference to grow deeper rather than longer toward equilibrium. Additionally, compressive residual stress up to 350 μm beneath the notch surface decreased mean stress via superposition of internal and external stresses resulting in further retardation of short crack growth, a well-documented phenomenon.[2,6,10,11,25–27] As a result, the crack growth rate remained somewhat constant with increasing $\Delta K_{Surface}$ values until 20 MPam$^{0.5}$. This was observed as suppressed crack initiation and coalescence activity between 40%–80% lifetime, not typically observed on non-peened U-notch samples. As the a/c ratio approached equilibrium and the crack grows past the compressive residual stress field, the short crack growth rate increased rapidly, approaching non-peened short crack growth rates.

Polished U-notch samples made from FV448 contained semi-elliptical crack shapes with higher a/c ratios than the theoretical equilibrium prediction under bending conditions. This higher a/c ratio is attributed to the presence of elongated stringers oriented perpendicular to the notch surface.[10] The FV566 U-notch samples contained a lower density of stringers and were oriented parallel to the tensile axis. The a/c ratios for both polished and shot peened samples without the influence of coalescence were found to be in agreement with theoretical equilibrium predicted values (Figure 15A). The a/c ratio reduced immediately following coalescence, which when allowed to develop unhindered will regain an a/c ratio based upon theoretical equilibrium (Figure 15B). In this instance, the a/c ratio can be approximated for the
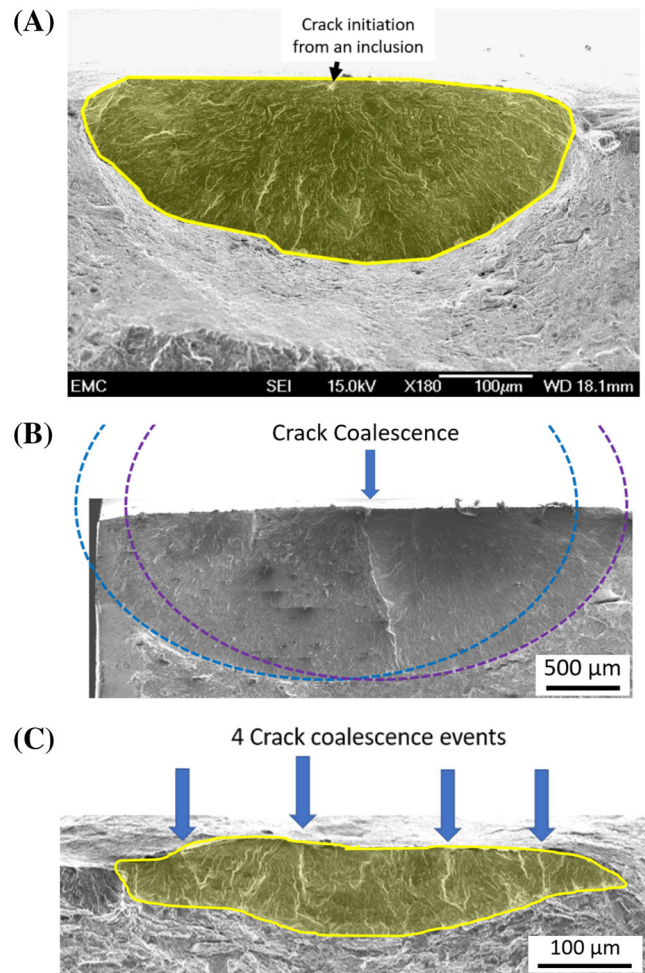
FIGURE 15 (A) A semi-elliptical fatigue region (shaded yellow) on the fracture surface of a polished U-notch sample with a/c ratio of 0.74 that has initiated from an inclusion. (B) Two semi-elliptical cracks that have coalesced and allowed to develop. (C) Four semi-elliptical cracks that have coalesced on a shot peened U-notch sample, forming a fatigue region shape with very low a/c ratio of approximately 0.3. [Colour figure can be viewed at wileyonlinelibrary.com]

individual cracks which tended to be overestimated compared with theoretical equilibrium. Particularly low a/c ratios were typically observed for short cracks less than 500 μm on shot peened surface conditions due to the high density of pre-existing cracks and subsequent early coalescence behavior leading to long surface cracks with particularly low a/c ratios (Figure 15C).

5 | CONCLUSIONS

FE modeling was used to investigate the effect of changing notch radius and notch depth on stress and strain range distribution and residual stress after unloading within the notch field. Changing the notch depth and

notch radius for the geometries tested did not significantly impact the distribution of stress, strain or residual stress within the notch field and did not affect short crack growth behavior. Depending upon sample geometry and loading conditions, changing the notch depth may influence the applied strain range, which had the largest effect on stress, strain, and residual stress within the notch field.

XRD on T0 shot peening U-notch samples found similar residual stress profiles to those observed previously in FV448 material.[9] Limitations in measurement angle may have reduced the accuracy of the residual stress profile in the longitudinal direction.

The number of initiation events for the primary crack increased with increasing strain range regardless of surface condition or notch geometry. Shot peening caused pre-existing cracks to form on the surface resulting in more crack initiation events, especially for the lower strain ranges tested.

Changing the notch geometry had a minimal effect on the short crack growth rate dc/dN versus $\Delta K_{Surface}$ based upon LEFM assumptions. On the other hand, the compressive residual stress induced by shot peening considerably retarded the surface crack growth rate by up to a factor of 10 and induced a period of low initiation and coalescence activity between 40% and 80% lifetime. The crack growth rate rapidly increased seemingly toward non-peened levels once short crack growth had surpassed the compressive residual stress region.

Semi-elliptical fatigue regions on polished U-notch samples typically suggested a/c ratios in agreement with theoretical equilibrium predictions. A high density of pre-existing cracks led to early multiple crack coalescence events resulting in atypical shallow semi-elliptical shapes with relatively low a/c ratios. The compressive residual stress induced from shot peening retarded crack growth in the depth direction reducing a/c ratios further.

T0 shot peening typically extended the total fatigue life of U-notch samples despite the increased surface roughness and presence of pre-existing cracks on the U-notch surface. The substantial retardation in the short crack growth rate was the main contributing factor in the lifetime extension attributed to compressive residual stress and strain hardening beneath the notch surface. The magnitude of the lifetime extension diminished with increasing strain range, lifetime extension from shot peening was no longer observed at strain ranges above 1.2% at the notch surface due to residual stress relaxation. This is also explained by our residual stress relaxation modeling approach below the notch root (Figure 7A,B). In bending notched samples, residual stress relaxation hardly occurs. But the gap between the shot-peening induced compressive residual stress and that generated by bending itself becomes diminished at higher load levels. Therefore, the benefits of shot peening will be swamped compared with lower strain levels.

NOMENCLATURE

FE/FEA	finite element/finite element analysis
FNC	Frazer-Nash Consultancy
LCF	low cycle fatigue
LEFM	linear elastic fracture mechanics
N-Depth	normalized depth
NDT	non-destructive testing
NF	notch field
PSBs	persistent slip bands
XRD	X-ray diffraction
P_{Max}	maximum load during baseload cycle
P_{Min}	minimum load during baseload cycle
a	the depth of a semi-elliptical surface crack
c	half the total length of a semi-elliptical surface crack
cproj	half projected length of a semi-elliptical surface crack length
dcproj/dN	projected surface crack growth rate
d	notch depth
ΔK	stress intensity factor range
$\Delta K_{Surface}$	stress intensity factor of semi-elliptical surface cracks
L_c	surface roughness gaussian cut-off filter
N	number of cycles
R_a	average surface height from the mean reference plane
W	depth of the sample
x	increasing depth from the notch surface
$\Delta \varepsilon$	strain range
σ_{max}	maximum stress
σ_{eff}	effective stress
σ_{yy}/σ_{22}	stress in the transverse direction
σ_{xx}/σ_{11}	stress in the longitudinal (tensile) direction
$\Delta \varepsilon_{xx}/\Delta \varepsilon_{11}$	strain range in the longitudinal direction
$\Delta \varepsilon_{yy}/\Delta \varepsilon_{22}$	strain range in the transverse direction

DATA AVAILABILITY STATEMENT

All data supporting this study are openly available from the University of Southampton repository at https://eprints.soton.ac.uk/476501/.

REFERENCES

1. Cunningham BMD, Evangelou A, You C, et al. Fatigue crack initiation and growth behavior in a notch with periodic overloads in the low-cycle fatigue regime of FV566 ex-service steam turbine blade material. *Fatigue Fract Eng Mater Struct*. 2022; 45(2):546-564.
2. He B. *Fatigue crack growth behaviour in a shot preened low pressure steam turbine blade material* [Thesis (Ph D) -]. University of Southampton, Faculty of Engineering and the Environment; 2015. Original typescript,; 2015
3. Pilkey WD, Pilkey DF, Bi Z. *Peterson's stress concentration factors*. John Wiley & Sons; 2020.
4. Liao D, Zhu SP, Correia JA, De Jesus AM, Berto F. Recent advances on notch effects in metal fatigue: a review. *Fatigue Fract Eng Mater Struct*. 2020;43(4):637-659.
5. Soady KA. *Reducing conservatism in life assessment approaches: industrial steam turbine blade to disc interfaces and the shot peening process* [Thesis (Eng D) -]. University of Southampton, Faculty of Engineering and the Environment; 2013. Original typescript; 2013
6. He BY, Soady KA, Mellor BG, Morris A, Reed PAS. Effects of shot peening on short crack growth rate and resulting low cycle fatigue behaviour in low pressure turbine blade material. *Mats Sci Technol*. 2013;29(7):788-796.
7. Soady KA, Mellor BG, West GD, Harrison G, Morris A, Reed PAS. Evaluating surface deformation and near surface strain hardening resulting from shot peening a tempered martensitic steel and application to low cycle fatigue. *Int J Fatigue*. 2013;54:106-117.
8. Xiang Y, Liu Y. Mechanism modelling of shot peening effect on fatigue life prediction. *Fatigue Fract Eng Mater Struct*. 2010; 33(2):116-125.
9. Soady KA, Mellor BG, Shackleton J, Morris A, Reed PAS. The effect of shot peening on notched low cycle fatigue. *Mater Sci Eng a*. 2011;528(29):8579-8588.
10. He BY, Soady KA, Mellor BG, Harrison G, Reed PAS. Fatigue crack growth behaviour in the LCF regime in a shot peened steam turbine blade material. *Int J Fatigue*. 2016;82:280-291.
11. You C, He BY, Achintha M, Reed PAS. Numerical modelling of the fatigue crack shape evolution in a shot-peened steam turbine material. *Int J Fatigue*. 2017;104:120-135.
12. Maiya PS, Busch DE. Effect of surface roughness on low-cycle fatigue behavior of type 304 stainless steel. *Metall Mater Trans a Phys Metall Mater Sci*. 1975;6(9):1761-1766.
13. Achintha M, You C, He BY, Soady K, Reed P. Stress relaxation in shot-peened geometric features subjected to fatigue: experiments and modelling. Paper presented at. *Adv Mater Res*. 2014; 996:729-735.
14. You C. *Fatigue lifing approaches for shot peened turbine components*. University of Southampton; 2017.
15. You C, Achintha M, Soady KA, Smyth N, Fitzpatrick ME, Reed PAS. Low cycle fatigue life prediction in shot-peened components of different geometries—part I: residual stress relaxation. *Fatigue Fract Eng Mater Struct*. 2017;40(5):761-775.
16. Turnbull A, Zhou S. Short Crack Growth Rates In a Steam Turbine Blade Steel. Paper presented at: CORROSION 20122012.
17. Institute BS. BS EN ISO 21920-3:2022 - Geometric product specifications (GPS) - Surface texture: profile. Part 3: Specification operators; 2022.
18. Cunningham BMD. *Extending Fatigue Life of Industrial Low-Pressure FV566 Turbine Blades: Efficacy of a Lifetime Extension Strategy to Extend Service Life* [Thesis (PhD) - University of Southampton, Faculty of Engineering and Physical Sciences]. University of Southampton; 2022.
19. Scott PM, Thorpe TW. A critical review of crack tip stress intensity factors for semi-elliptic cracks. *Fatigue Fract Eng Mater Struct*. 1981;4(4):291-309.
20. Holdbrook SJ, Dover WD. The stress intensity factor for a deep surface crack in a finite plate. *Eng Fract Mech*. 1979;12(3):347-364.
21. Guagliano M, Vergani L. An approach for prediction of fatigue strength of shot peened components. *Eng Fract Mech*. 2004; 71(4–6):501-512.
22. Zinn W, Scholtes B. Influence of shot velocity and shot size on Almen intensity and residual stress depth distributions. Paper presented at: Proceedings of the 9th International Conference on Shot Penning. Paris, France; 2005.
23. Saklakoglu N, Bolouri A, Irizalp SG, Baris F, Elmas A. Effects of shot peening and artificial surface defects on fatigue properties of 50CrV4 steel. *Int J Adv Manuf Technol*. 2021;112(9): 2961-2970.
24. Sakamoto J, Lee Y, Cheong S. Effect of surface flaw on fatigue strength of shot-peened medium-carbon steel. *Eng Fract Mech*. 2015;133:99-111.
25. Soady K. Life assessment methodologies incoroporating shot peening process effects: mechanistic consideration of residual

stresses and strain hardening part 1–effect of shot peening on fatigue resistance. *Mats Sci Technol.* 2013;29(6):637-651.

26. Sanchez AG, You C, Leering M, et al. Effects of laser shock peening on the mechanisms of fatigue short crack initiation and propagation of AA7075-T651. *Int J Fatigue.* 2021;143: 106025.

27. You C, Achintha M, He BY, Reed PAS. A numerical study of the effects of shot peening on the short crack growth behaviour in notched geometries under bending fatigue tests. *Int J Fatigue.* 2017;103:99-111.